Published in final edited form as:
IEEE Trans Neural Syst Rehabil Eng. 2008 February ; 16(1): 37–45. doi:10.1109/TNSRE.2007.910282.

An Analysis of EMG Electrode Configuration for Targeted Muscle Reinnervation Based Neural Machine Interface

He Huang [Member, IEEE],
Neural Engineering Center for Artificial Limbs, Rehabilitation Institute of Chicago, IL, 60611

Ping Zhou [Senior Member, IEEE],
Neural Engineering Center for Artificial Limbs, Rehabilitation Institute of Chicago, IL, 60611. Department of Physical Medicine and Rehabilitation, Northwestern University, Chicago, IL, 60611, USA

Guanglin Li [Senior Member, IEEE], and
Neural Engineering Center for Artificial Limbs, Rehabilitation Institute of Chicago, IL, 60611. Department of Physical Medicine and Rehabilitation, Northwestern University, Chicago, IL, 60611, USA

Todd A. Kuiken [Senior Member, IEEE]
Neural Engineering Center for Artificial Limbs, Rehabilitation Institute of Chicago, IL, 60611. Department of Physical Medicine and Rehabilitation, Northwestern University, Chicago, IL, 60611, USA

Abstract

Targeted muscle reinnervation (TMR) is a novel neural machine interface for improved myoelectric prosthesis control. Previous high-density (HD) surface electromyography (EMG) studies have indicated that tremendous neural control information can be extracted from the reinnervated muscles by EMG pattern recognition (PR). However, using a large number of EMG electrodes hinders clinical application of the TMR technique. This study investigated a reduced number of electrodes and the placement required to extract sufficient neural control information for accurate identification of user movement intents. An electrode selection algorithm was applied to the HD EMG recordings from each of 4 TMR amputee subjects. The results show that when using only 12 selected bipolar electrodes the average accuracy over subjects for classifying 16 movement intents was 93.0(±3.3)%, just 1.2% lower than when using the entire HD electrode complement. The locations of selected electrodes were consistent with the anatomical reinnervation sites. Additionally, a practical protocol for clinical electrode placement was developed, which does not rely on complex HD EMG experiment and analysis while maintaining a classification accuracy of 88.7±4.5%. These outcomes provide important guidelines for practical electrode placement that can promote future clinical application of TMR and EMG PR in the control of multifunctional prostheses.

Corresponding author: T. Kuiken (Phone: 01-312-238-1315, Fax: 01-312-238-2081, tkuiken@northwestern.edu).

Index Terms

Targeted muscle reinnervation; EMG; clinical EMG electrode configurations; control of artificial limbs; prosthesis; classification

I. Introduction

For decades surface electromyography (EMG) has been widely applied as a control source for upper-limb prostheses [1]–[5]. In current practice, either the position or the speed of a motor in the prosthesis is controlled by the magnitude of EMG signals recorded from one or two residual muscles. Unfortunately, this is inadequate for high-level injuries such as transhumeral and higher amputations; the user must sequentially control each available prosthetic component (hand, wrist, and elbow), a process that is slow and cumbersome. Furthermore, controlling multiple prosthetic joints by activating anatomically unrelated muscles creates a significant mental burden for the amputee. Recently, with advancements in microprocessor and signal processing technology, pattern recognition (PR) based multifunctional myoelectric prostheses have been proposed [6]–[9]. Unfortunately, PR systems are not applicable for patients with transhumeral amputation and higher because too few residual muscles remain from which to extract control signals.

To address this challenge, our research group has developed a new neural machine interfacing (NMI) technology called targeted muscle reinnervation (TMR), which improves control of multifunctional myoelectric upper-limb prostheses [10], [11]. Neural information that controlled the limb prior to amputation remains in the residual peripheral nerves. TMR offers access to these control signals via surface EMG by surgically transferring the residual nerves to alternative residual muscles that are no longer biomechanically functional [10]–[13]. Successful TMR allows voluntary motor control signals that used to activate muscles in the amputated limb to activate these newly reinnervated muscles. The resultant EMG signals can be used to drive the artificial limb. Four individuals with transhumeral or shoulder disarticulation amputations have received successful TMR surgery. Four pairs of bipolar EMG electrodes mounted in the prosthetic socket captured myoelectric signals from the reinnervated muscles for proportional control of hand open/close and elbow extension/flexion. Previous studies reported that subjects performed the box and blocks and clothes pin functional task 2.5–7 times faster when using their experimental TMR prostheses than when using conventional myoelectric prostheses [10], [11], [13]. Subjectively, they felt the TMR prosthesis control was easier and more intuitive.

In addition to elbow extension/flexion and hand open/close, the transferred nerves normally innervate dozens of muscles for actuating all the movements of elbow, wrist, and hand. This inspired us to hypothesize that the EMG signals from TMR muscles may contain more dormant neural control contents of the missing limb and might potentially be used to control more functions in a prosthesis. A prior study has shown that a great amount of neural control contents can be extracted from TMR muscles with pattern recognition (PR) methods [14]. While four TMR amputees attempted to perform 16 different arm movements as if their amputated arm was present, the EMG signals were recorded over their reinnervated muscles using a high density (HD) electrode array of 116–128 monopolar electrodes. Using the time

domain (TD) features of bipolar EMG signals, a simple linear discriminant analysis (LDA) could classify the 16 movement intents, including movements of the elbow, wrist, individual fingers and thumb, with 96.0±3.9% accuracy averaged over four subjects.

The results from the HD EMG study are encouraging. However, it is clinically challenging to place more than 100 electrodes under a prosthetic socket. In addition it is technically demanding to base prosthesis control on real-time PR with a large number of EMG signal inputs. This raises the question of whether most of the motor control contents could be derived from the surface EMG signals captured by a limited number of electrodes. A positive answer will be essential for the application of the TMR technique in multifunctional myoelectric prosthesis control.

In this study, we developed an electrode selection algorithm for the HD EMG recordings, which suboptimally selected a reduced number of electrodes required to preserve sufficient neural control information for accurate classification of user movement intents. The placement of selected electrodes was identified as the suboptimal configuration and the temporal stability of information extraction was also investigated. Moreover, we tested two additional electrode configurations that can be implemented without analyzing HD EMG and compared their capability of information extraction to that of the suboptimal configuration. This is because performing HD EMG experiments and analysis is not practical for clinics; the required equipment, time, and expertise needed for these experiments are beyond means of prosthetist today. If a simpler configuration could extract sufficient neural information as well with a reduced electrode number, this study would allow us to establish guidelines to facilitate future clinical applications of EMG electrode placement over TMR muscles without using HD EMG experiments.

II. Methods

A. Participants and Targeted Muscle Reinnervation

Targeted muscle reinnervation surgery and this study were approved by the ethics committee and written informed consent was obtained from all subjects. Four people with TMR surgeries participated in this study: one male subject with bilateral shoulder disarticulations (S1), one female with unilateral short transhumeral amputation (S2), and two males with unilateral long transhumeral amputations (S3 and S4). Fig. 1 (left panel) illustrates schematically the TMR procedure in S2 (a) and in S3 and S4 (b). Using S3 as an example, during TMR surgery the medial head of the biceps and brachialis muscle were denervated. The median nerve was transferred to the medial biceps and the distal radial nerve was transferred to the brachialis. Muscle reinnervation was observed 4 months after surgery. When S3 thought to close his hand or flex his wrist, the medial biceps would contract. When he thought to open his hand or extend his wrist, the brachialis muscle would contract. The lateral biceps and triceps were still available to produce EMG signals for elbow flexion and extension, respectively. Detailed information about TMR surgical procedures and clinical results has been presented in [10]–[13].

B. High Density EMG Experiments and Data Collection

The HD EMG recordings were conducted on all four subjects. EMG signals were captured by placing a grid of 116–128 monopolar surface electrodes over TMR muscles and the biceps and triceps muscles, if present. A reference electrode was located on the bony area of shoulder. The distance between electrodes was 15~20 mm [15]. A BioSemi system (BioSemi Active II System, Amsterdam, Netherlands) was used to record HD EMG signals at a sampling rate of 2048 Hz. The cut-off frequency of the anti-aliasing filter was one fifth of the sampling rate (409.6 Hz). Sixteen movements were involved in this study. Eight of these movements were basic joint motions that are offered in commercially available upper-limb prostheses, namely elbow flexion/extension, wrist flexion/extension, pronation/supination, and hand open/close. The other eight were thumb adduction/abduction, thumb flexion/extension, index finger flexion/extension, and 3^{rd}~5^{th} finger flexion/extension. Subjects were asked to watch a video demonstration of each movement and to imagine moving their absent limb in synchrony with the video. An experimental trial contained 10 repetitions of one type of movement. For each repetition, the subjects were asked to exert a comfortable level of contraction at a medium force, to hold the contraction for approximately 5 seconds, and then to relax for the next 5 seconds. To avoid muscle and mental fatigue, the subjects were allowed 3 to 5 minutes' rest between trials.

C. EMG Pre-processing Pattern Recognition Method

A sixth order Butterworth high-pass filter with a 5 Hz cutoff frequency was applied on EMG signals to remove motion artefacts [16]. As bipolar EMG allow a more focal recording area and are more clinically relevant than monopolar recordings, the bipolar EMG signals (*BEMG*) were used and were derived by

$$BEMG_{ij} = MEMG_i - MEMG_j, \quad (1)$$

where *MEMG* denotes a monopolar EMG signal and the *i* and *j* monopolar electrodes are spatially nearest neighbours. Here, each combination of two neighbouring monopolar electrodes was termed a bipolar EMG electrode. The relationship between two neighbouring electrodes could be longitudinal, latitudinal, or diagonal.

This study used four EMG TD features and LDA to identify user intent because of their simplicity and reliable performance [7]. Previous studies showed that four TD features (the mean absolute value, the number of zero-crossings, the waveform length, and the number of slope sign changes) could extract the information in the EMG signals and were fast to calculate [7], [17]. The detailed equation and description of these four TD features can be found in [7], [14]. Additionally, studies reported that the simple LDA classifier produced a similar classification performance compared to other more complex types [7], [18]. The LDA-based EMG PR algorithm is described in the Appendix. To quantify the performance of the classifier, the classification accuracy (*CA*) was calculated by

$$CA = \frac{Number\ of\ correctly\ classified\ samples}{Total\ number\ of\ testing\ samples} \times 100\%. \quad (2)$$

D. Electrode Selection Algorithm

Based on (1), the number of bipolar EMG electrodes derived from the HD array was 402 for S1, 440 for S2, 407 for S3, and 426 for S4, which is too high for clinical practice. An electrode selection algorithm based on the Sequential Forward Searching (SFS) method [19] was developed to select a limited number of electrodes that contain most of neural control information for reliable classification. The procedure of SFS is described as follows.

Step 1: Two electrode sets were initialized: the applied electrode set A that contains the selected electrodes was initially empty (A=Ø, m=0), and the remaining electrode set R included all bipolar EMG electrodes derived from the HD array (R={r_1, r_2, …, $r_{N_{HD}}$}, n=N_{HD}). *r* denotes an electrode in set R and *a* denotes an electrode in set A.; m and n denote the number of electrodes in set A and set R respectively.

Step 2: In the first searching iteration, the TD features of each individual bipolar electrode in set R were used to train and test a LDA classifier. The electrode that produced the maximum classification accuracy as in (3) was chosen as the first selected electrode.

$$r_k = \arg\max_{r_i}\{CA_{r_i} : CA_{r_i} = f_{CA}(r_i) for\ r_i \in R\}, \quad (3)$$

where the classification accuracy is described as a function of applied electrodes *r*, i.e. $CA_r = f_{CA}(r)$. Then, r_k was removed from set R ($R = R\backslash\{r_k\}$, n=N_{HD}−1) and added into set A ($A=\{a_1 = r_k\}$, m=1). Additionally, we calculated the normalized classification accuracy (*nca*) defined as

$$nca = \frac{CA_A}{CA_{HD}} \times 100\%, \quad (4)$$

where CA_{HD} is the classification accuracy as a result of using all bipolar electrodes derived from the HD electrode array, and CA_A is the accuracy when using the selected electrodes in the updated set A.

Step 3: In the following iterations, we paired each of the remaining electrodes in set R with all previously searched electrodes in set A, i.e. $A \cup \{r_i\}$, and applied these electrodes to train and test a classifier. The electrode in set R paired with the electrodes in set A that generated the maximum *CA* as in (5) was identified and moved to electrode set A from set R.

$$r_k = \arg\max_{r_i}\{CA_{A\cup\{r_i\}} : CA_{A\cup\{r_i\}} = f_{CA}(A \cup \{r_i\}) \text{ for } r_i \in R\}. \quad (5)$$

The set A and set R were then updated as

$$A=A\cup\{r_k\},\quad m=m+1,\quad \text{and}\quad R=R\backslash\{r_k\}, n=n-1.$$

In each iteration, one electrode in set R was selected and added into set A as the most informative electrode. The *nca* improved when the number of selected electrodes in the set A increased. Two criteria could be applied to terminate the iteration: (1) *nca* ≥ *nca_th*, and (2) m> *N_th*, where *nca_th* was the threshold of normalized classification accuracy ranging from 0% to 100% and *N_th* was the threshold of applied electrode number in set A.

Note that, ideally, all combinations of the total applied bipolar electrodes (N_{HD}) taken m at a time, i.e. ($\binom{m}{N_{HD}}$), should be examined in order to select the optimal m electrodes for maximum classification accuracy. However, such an exhaustive search was impossible for the current computational system. SFS searches electrodes suboptimally with much reduced searching time. The number of analyzed electrode combinations is $N_{HD}+(N_{HD}-1)+\ldots+(N_{HD}-m+1)$. For example, if m=10 and N_{HD}=400, the number of analyzed combinations is $\binom{10}{400}=2.58\times10^{19}$ for the exhaustive search, while it is only 3955 for SFS method. In the case of N_{HD} =400, unless m=1 or m≥398, the number of searched electrode combinations in SFS is much less than that in the exhaustive search. Hence, the placement of SFS-searched electrodes was named the Suboptimal Configuration.

E. Analysis of the Temporal Stability of the Suboptimal Configuration

The temporal stability of the SFS-selected electrodes was further validated using the EMG data recorded from follow-up EMG experiments on two subjects (S1 and S2), which were performed three to four months after the first experiments. The Suboptimal Configuration of the SFS-selected electrodes determined in the first EMG experiment was used in the follow-up experiment. The experimental protocol was the same as the first experiment. Using the EMG signals from these SFS-selected electrodes, we trained and tested the LDA classifier to decipher the 16 movement intents of the subjects.

F. Geometrical and Clinical Electrode Configurations

Two electrode configurations with the same number of electrodes as in the Suboptimal Configuration were tested. These configurations do not require a HD EMG experiment and SFS analysis to determine the electrode placement. By comparing classification accuracy of these two electrode configurations with that of the Suboptimal Configuration, we can (1) determine the relative efficacy of these configurations in neural information extraction, (2) test the spatial sensitivity of the classification accuracy to the EMG electrode placement, and (3) identify the electrode placement configuration that would provide reliable and easy clinical application.

The Geometrical Configuration was selected by approximating a uniform placement of applied bipolar EMG electrodes over the targeted muscles. An example for S2 is shown in Fig. 2a, in which 12 electrodes were assumed to be applied. No prior SFS analysis of the HD

EMG or clinical measurement was required. The Geometrical Configuration is the simplest of the three studied configurations to design and implement.

The Clinical Configuration was determined based on the extent of anatomical knowledge and clinical understanding of each subject's TMR surgery. It is relatively easy for a prosthetist to determine the point of maximal EMG signal amplitude over each of the target muscle by readily available tools [20]. We hypothesize that these locations would contain a great amount of neural control contents and could serve to guide clinical electrode placement. Fig. 2b demonstrates an example of a Clinical Configuration for S2. First, the 4 direct control sites were selected. These sites had the largest EMG amplitude for each nerve transfer and were functionally independent [20] (purple electrodes in Fig. 2b). These EMG signals from 4 direct control sites, designated as D1/D3 and D2/D4 (Fig. 2b), have been used to proportionally control the hand close/open and elbow flexion/extension functions in the subject's prosthesis. Eight additional electrodes (in green) were located over specifically involved muscles, especially those reinnervated by nerves that originally controlled multiple joints—the median and radial nerves. In general, they were clustered over the central regions of the reinnervated muscles with large EMG amplitude. All bipolar clinical electrodes were oriented parallel to the estimated direction of the underlying muscle fibers. For subjects S1 and S2, the *pectoralis major* was used for TMR. The estimated direction of these muscle fibers was from the muscle's origin to insertion (Fig. 2). For long transhumeral amputees S3 and S4, the muscles in the residual upper arm were used. Bipolar electrodes were placed parallel to the residual humerus. Taking advantage of the uniform electrode orientation in S3 and S4 in Clinical Configuration, we also compared the effects of electrode orientation on the extraction of neural information by alternately covering the same spots with electrodes placed in longitudinal, latitudinal and diagonal orientations. The selection of the Clinical Configuration was blind to the Suboptimal Configuration.

III. Results

A. Performance of Electrode Selection Algorithm

The SFS was tested on two classifiers: an 8-movement classifier of the basic joint movements and a 16-movement classifier that recognized the 8 basic joint movements plus an additional 8 finger and thumb movements. For the 16-movement classifier, if $nca \geq 98\%$ was applied as a criterion to stop the SFS iteration, the number of suboptimal selected electrodes was 11 bipolar electrodes for S1, 12 for S2, 10 for S3, and 11 for S4. That is to say, only 12 or less suboptimal placed EMG electrodes could extract essentially as much neural control information as the entire 402–440 differential recordings possible from the HD EMG experiments. For easy comparison among subjects, the number of selected electrodes (N_th) was set to 12 for all four subjects and $m > N\_th$ was used to terminate the SFS iteration.

Fig. 3 demonstrates the relationship between the number of SFS-selected suboptimal electrodes and the corresponding classification accuracy when using these suboptimal electrodes. Accuracy for the 16-movement classifier (Fig. 3a) increases dramatically at the beginning of the curve. The first five selected electrodes provide 77%–87% accuracies for all four subjects. When using 12 suboptimal bipolar electrodes, the average classification

accuracy over four subjects is 93.0(±3.3)%, only 1.2% lower that when using HD EMG recordings. The 8-movement classifier demonstrated a similar trend (Fig. 3b). The classification accuracy quickly reached a plateau. Classification accuracies of greater than 90% could be achieved in all subjects with just 6 bipolar electrodes. With 12 electrodes, the averaged classification accuracy over the four subjects was 99.1(±0.8)%, only 0.2% lower than when using HD EMG recordings.

B. Temporal Stability of Suboptimally Selected Electrodes

The 12 electrode Suboptimal Configurations for S1 and S2 gave very similar classification accuracies with repeated experiments. The accuracy of classifying 16 classes of movements was 96.2% in the first experiment for subject S1 and 96.3% in the experiment repeated 4 months later. For subject S2, the initial experiment had a classification accuracy of 88.6% and the second experiment 3 months later produced an accuracy of 90.4%.

C. Suboptimal Electrode Location

Fig. 4 demonstrates the Suboptimal Configuration on subjects S2 and S4 using a 16-movement classifier from the original HD EMG electrode configuration. Fig. 4b expands the 3-dimensional HD electrode array that wrapped around S4's transhumeral residual limb into a 2-dimensional plot, allowing better visualization. The purple rectangles in the background indicate direct control sites as points of reference. The green electrodes (Suboptimal Configuration) are the electrodes selected by the SFS algorithm. The label beside each electrode denotes the sequence of electrode selection during the sequential forward search.

At least one electrode in the Suboptimal Configuration was on or partially collated with a direct control site. For instance, in the results for S2 (Fig. 4a), the 5^{th}, 7^{th}, and 9^{th} suboptimal electrodes directly overlaid the control sites D4, D1, and D2, respectively, and the 8^{th} and 10^{th} electrodes overlaid the site D3. Additionally, in the Suboptimal Configuration the majority of the first 12 electrodes selected were clustered over the TMR muscles reinnervated by the median and radial nerves which previously controlled the hand and wrist. For S2 (Fig. 4a), 5 out of 12 of the first electrodes assigned were located at the *serratus* reinnervated by the radial nerve, while 3 electrodes were over the sternal head of the *pectoralis* reinnervated by the median nerve. Interestingly, one electrode was located over the portion of the clavicular head reinnervated by the ulnar nerve. A similar result is seen in S4 (Fig. 4b). The majority of the first 12 suboptimal electrodes were clustered at the *brachialis* reinnervated by the radial nerve and at the *biceps* whose medial head was innervated by the median nerve.

D. Comparison of Classification Accuracy of Suboptimal, Clinical and Geometric Configurations

The comparison of 16-movement classification accuracy using electrodes placed according to Suboptimal, Clinical, and Geometrical Configurations is demonstrated in Fig. 5 with representative data from S4. Compared to the Clinical Configuration and Geometric Configuration, the SFS-selected electrodes (Suboptimal Configuration) always provided the highest accuracy. Using the Clinical and Geometrical Configurations, classification accuracy also improved as the number of applied electrodes increased. However, compared to the

curve of Suboptimal Configuration, the Clinical and Geometric Configurations did not show the rapid improvement and quick achievement of a plateau. This is because the sequence of electrode selection was assigned subjectively in the Clinical and Geometrical Configurations. When using 6 electrodes, the classification accuracies of both the Clinical and Geometric Configurations were more than 15% lower than that of the Suboptimal Configuration. This result implies that when the number of applied electrodes is small (<6), the electrode selection is critical for the 16-movement classifier's performance. When more EMG electrodes are added, the classification accuracy using the Clinical Configuration is higher than that using the Geometrical Configuration and approaches the accuracy of the Suboptimal Configuration. Furthermore, Fig. 5 also shows the effect of electrode orientation on the classification accuracy. In the Clinical Configuration, classification accuracy is similar among longitudinal, latitudinal, and diagonal electrode orientations. This finding indicates that EMG electrode orientation does not influence the extraction of neural information.

These observations are also true for the other subjects as shown in Fig. 6. When using 12 EMG electrodes to classify 16 movement classes, the average classification accuracy over the four subjects was 93.0±3.3% for the Suboptical Configuration, 88.7±4.5% for the Clinical Configuration, and 72.9±8.6% for the Geometric Configuration.

IV. Discussion

Results from this study show that 12 or less EMG electrodes placed over TMR and other residual muscles can pick up neuromuscular control information for the amputated limb, including the control of finger movements. This electrode number is clinically feasible for myoelectric prosthesis control when considering current socket design, electrode hardware, and the power of current microprocessors. Using 12 suboptimally selected electrodes, the LDA classified the basic 8 movement classes with 99.1% accuracy. This indicates that individuals with transhumeral or shoulder disarticulation amputations could reliably control a prosthesis with a powered elbow, wrist rotator, wrist flexion unit, and hand. This is beyond the current capability of commercially available prostheses which do not include powered wrist flexion. The 16-class analysis was more challenging as it included 8 additional movements involving the thumb and fingers. Yet high classification accuracy was still achieved with a 93.0% average over all subjects. These results suggest the clinical feasibility of TMR and EMG PR-based control for more complex prostheses with two degree of freedom wrists and multifunction hands, such as those under development in the Defense Advanced Research Agency's Revolutionizing Upper Limb Prosthetics Program and elsewhere [21], [22]. This will provide potential for significantly improving the function of prostheses for people with transhumeral and shoulder disarticulation amputation.

The SFS electrode selection algorithm applied to HD EMG recordings is a computationally efficient and useful way to obtain a Suboptimal Configuration of electrode placement for maximal neural information extraction. Compared to the other electrode configurations explored in this study, the placement of EMG electrodes in the Suboptimal Configuration produced the highest classification accuracy. The SFS algorithm placed the majority of electrodes over the central portions of muscles reinnervated by the median and radial nerves.

This highlights that most of the control content involving the distal joints is transmitted through the median and radial nerves. Interestingly, in S2, the suboptimal electrodes were assigned to the area of the *pectoralis* that had been reinnervated by the ulnar nerve, although ulnar reinnervation did not elicit a strong, isolated muscle signal for direct control of a prosthetic component [10].

In order to accurately classify multiple functions, the SFS algorithm selected several spatially separated electrodes in one reinnervated muscle territory. This suggests that TMR gives rise to discrete, spatial segregation of motor activation within a single reinnervated muscle. In our previous study, we also observed that in S1 two strong activations at different spots within one muscle reinnervated by the median nerve were correlated separately with hand close and thumb abduction [10]. Both of these observations imply that there is some functional organization in the proximal amputated nerve that is maintained to some degree as the motor axons regenerate through the muscle and reinnervate muscle fibers.

The analysis of suboptimal electrode placement showed that most of the neural information available could be extracted with a greatly reduced number of electrodes. However, it was unclear how precisely the electrodes needed to be placed to obtain high classification accuracy. Furthermore, the HD EMG experiments, if necessary, would be a significant obstacle to clinic success of PR-based control. Therefore, a Geometric Configuration was analyzed to test the sensitivity of electrode placement and to determine if this very simple configuration would be clinically viable. Unfortunately, the classification accuracy averaged over subjects for 16 movements was only 72.9%. This implies that a small number of electrodes evenly spaced over the target muscles do not capture sufficient information content for high classification accuracy and electrode location is very import for efficient extraction of neural information. Thus, this simple method of applying electrodes would be inadequate for clinical use.

However, we can estimate the areas where most of neural control information was located based on the clinical understanding of each subject’s TMR surgery and place electrodes over these areas as shown in the Clinical Configuration. The average classification accuracy when using the Clinical Configuration is only 4.3% lower than that found when using the Suboptimal Configuration. Additionally, the electrode placement of the Clinical Configuration and that of Suboptimal Configuration were similar, indicating that the Suboptimal Configuration of electrode placement is consistent with the anatomical nerve-muscle transfer arrangement. Importantly, this result implies that some rules of electrode placement can be followed for effective neural control information extraction in a clinical setting--without the use of complex HD EMG experiments and the SFS algorithm.

Based on the results of the EMG electrode configurations explored in this study, we offer simple guidelines for effective electrode placement, even without HD EMG recordings. These guidelines will facilitate future clinical application of TMR and PR-based myoelectric prosthetic control. A good starting point is to locate electrodes near sites where high EMG magnitude can be obtained. For robust application, electrodes with high signal levels have better tolerance to high noise levels. Furthermore, these sites likely lie in the centers of reinnervated muscles where signal content is greatest. The locations of clinical electrodes

should cover all functional muscles necessary to control the particular joint movements. Based on knowledge of each subject's TMR surgical outcome, clinicians are urged to apply more electrodes over muscles that embed the most motor control information, in particular the median and distal radial nerve regions. A small number of electrodes (possibly only one) should be sufficient for the musculocutaneous target muscle (which only controls elbow flexion) or residual native muscles like the biceps and triceps. It is important to note that as the number of applied electrodes decreases, exact electrode placement becomes increasingly important for better classification accuracy. Hence, within the constraints of the system, more EMG electrodes were preferred in clinical application for more reliable pattern recognition. Although the orientation of electrodes does not greatly affect the accuracy of movement intent classification (Fig. 5), it is recommended that electrodes be aligned along the estimated direction of the muscle fibers, which offers large signal levels and better tolerance to noise [15].

The electrode stability analysis addresses one of the important issues of clinical feasibility. The control system must have some tolerance for variability of electrode placement. It is not possible to place the electrodes in exactly the same position every time the prosthesis is donned. The validation analyses presented in this study indicates that high pattern classification accuracy can be obtained in repeated experiments where there has been at least some movement of the suboptimally placed electrodes. However, this analysis was performed on only two sets of experiments, thus it should be considered preliminary work.

More research on the robustness of a real-time pattern recognition control system with TMR is needed, such as in keeping electrodes stably located over muscles, in how to quickly and robustly train the classifiers, in building an easy interface for clinicians, and in developing training protocols for patients. In addition, prostheses are needed which are more dexterous than those commercially available today. This work adds to the growing body of literature showing that we can control multifunction shoulders, elbows, wrists and complex prosthetic hands [21], [22].

V. Conclusions

In conclusion, this study provides evidence and tools for the clinical implementation of a multifunctional prosthetic control strategy that combines TMR and EMG pattern recognition. The information involved in the control of movement of a missing arm and hand can be extracted using a practical and clinically feasible number of EMG electrodes placed over reinnervated muscles and other residual muscles. This study explores the configurations of electrode placement, and initial guidelines of effective electrodes placement are offered for future clinical application of TMR and EMG PR in myoelectric prosthesis control.

Acknowledgments

This work was supported by the NIH National Institute of Child and Human Development (Grants # R01 HD043137-01, #R01 HD044798 and # NO1-HD-5-3402), the Defense Advanced Research Projects Agency, and U.S. Department of Education, the National Institute on Disability and Rehabilitation Research (Grant # H133F060029).

We would like to thank Kevin Englehart, Ph.D., Levi Hargrove, M.S., Aimee Schultz, M.S., Paul Marasco, Ph.D. and. R. J. Garrick, Ph.D. for assistance with this manuscript.

References

1. Hogan N. A review of the methods of processing EMG for use as a proportional control signal. Biomed Eng. 1976; 11:81–6. [PubMed: 1252567]
2. Philipson L, Childress DS, Strysik J. Digital approaches to myoelectric state control of prostheses. Bull Prosthet Res. 1981; 10–36:3–11. [PubMed: 19594448]
3. Parker PA, Scott RN. Myoelectric control of prostheses. Crit Rev Biomed Eng. 1986; 13:283–310. [PubMed: 3512166]
4. Sears HH, Shaperman J. Proportional myoelectric hand control: an evaluation. Am J Phys Med Rehabil. 1991; 70:20–8. [PubMed: 1994966]
5. Williams TW 3rd. Practical methods for controlling powered upper-extremity prostheses. Assist Technol. 1990; 2:3–18. [PubMed: 10149040]
6. Ajiboye AB, Weir RF. A heuristic fuzzy logic approach to EMG pattern recognition for multifunctional prosthesis control. IEEE Trans Neural Syst Rehabil Eng. 2005; 13:280–91. [PubMed: 16200752]
7. Englehart K, Hudgins B. A robust, real-time control scheme for multifunction myoelectric control. IEEE Trans Biomed Eng. 2003; 50:848–54. [PubMed: 12848352]
8. Chu JU, Moon I, Mun MS. A real-time EMG pattern recognition system based on linear-nonlinear feature projection for a multifunction myoelectric hand. IEEE Trans Biomed Eng. 2006; 53:2232–9. [PubMed: 17073328]
9. Peleg D, Braiman E, Yom-Tov E, Inbar GF. Classification of finger activation for use in a robotic prosthesis arm. IEEE Trans Neural Syst Rehabil Eng. 2002; 10:290–3. [PubMed: 12611366]
10. Kuiken TA, Dumanian GA, Lipschutz RD, Miller LA, Stubblefield KA. The use of targeted muscle reinnervation for improved myoelectric prosthesis control in a bilateral shoulder disarticulation amputee. Prosthet Orthot Int. 2004; 28:245–53. [PubMed: 15658637]
11. Kuiken T. Targeted reinnervation for improved prosthetic function. Phys Med Rehabil Clin N Am. 2006; 17:1–13. [PubMed: 16517341]
12. Hijjawi JB, Kuiken TA, Lipschutz RD, Miller LA, Stubblefield KA, Dumanian GA. Improved myoelectric prosthesis control accomplished using multiple nerve transfers. Plast Reconstr Surg. 2006; 118:1573–8. [PubMed: 17102730]
13. Kuiken TA, Miller LA, Lipschutz RD, Lock BA, Stubblefield K, Marasco PD, Zhou P, Dumanian GA. Targeted reinnervation for enhanced prosthetic arm function in a woman with a proximal amputation: a case study. Lancet. 2007; 369:371–80. [PubMed: 17276777]
14. Zhou P, Lowery MM, Englehart KB, Huang H, Li G, Hargrove L, Dewald JPA, Kuiken T. Decoding a new neural-machine interface for control of artificial limbs. J Neurophysiol. 2007
15. Hermens HJ, Freriks B, Disselhorst-Klug C, Rau G. Development of recommendations for SEMG sensors and sensor placement procedures. J Electromyogr Kinesiol. 2000; 10:361–74. [PubMed: 11018445]
16. Merletti, R.; Parker, P. Electromyography : physiology, engineering, and noninvasive applications. Hoboken, NJ: IEEE/John Wiley & Sons; 2004.
17. Hudgins B, Parker P, Scott RN. A new strategy for multifunction myoelectric control. IEEE Trans Biomed Eng. 1993; 40:82–94. [PubMed: 8468080]
18. Hargrove LJ, Englehart K, Hudgins B. A comparison of surface and intramuscular myoelectric signal classification. IEEE Trans Biomed Eng. 2007; 54:847–53. [PubMed: 17518281]
19. Somol P, Pudil P, Novovicova J, Paclik P. Adaptive floating search methods in feature selection. Pattern Recognition Letters. 1999; 20:1157–63.
20. Lipschutz, RD. Upper extremity amputations and prosthetic management. In: Nielsen, CC., editor. Orthotics and Prosthetics in Rehabilitation. Boston: Butterworth-Heinemann Publications; 2000.
21. Carrozza MC, Cappiello G, Micera S, Edin BB, Beccai L, Cipriani C. Design of a cybernetic hand for perception and action. Biol Cybern. 2006; 95:629–644. [PubMed: 17149592]

22. Kyberd PJ, Chappell PH. The Southampton Hand: an intelligent myoelectric prosthesis. J Rehabil Res Dev. 1994; 31:326–34. [PubMed: 7869280]

23. Duda, RO.; Hart, PE.; Stork, DG. Pattern classification. 2. New York: Wiley; 2001.

Biographies

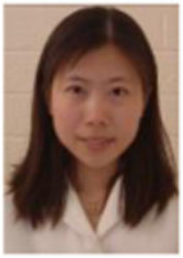

He Huang (M'06) received a B.S. from the School of Electronics and Information Engineering at Xi'an Jiao-Tong University, China and a M.S. and Ph.D. degree from the Harrington Department of Bioengineering, Arizona State University. She is currently a research associate in the Neural Engineering Center for Artificial Limbs at the Rehabilitation Institute of Chicago.

Her primary research interests include neural-machine interface, modeling and analysis of neuromuscular control of movement in normal and neurologically disordered humans, virtual reality in neuromotor rehabilitation, and design and control of therapeutic robots, orthoses, and prostheses. Her specialties lie in signal and image processing, machine learning, adaptive control, biomechanical modeling, and motion analysis.

Ping Zhou received the B.S. degree in Electrical Engineering and M.S. degree in Biomedical Engineering from University of Science and Technology of China, Hefei, China, in 1995 and 1999 respectively, and a Ph.D. degree in Biomedical Engineering from Northwestern University, Evanston, USA, in 2004. After that he did two years' postdoctoral research at the Rehabilitation Institute of Chicago, Chicago, USA.

He is currently a Research Scientist with the Rehabilitation Institute of Chicago, Chicago, USA and a Research Assistant Professor with the Department of Physical Medicine and Rehabilitation, Northwestern University, Chicago, USA. His research interests include motor unit recording and analysis, biomedical signal (in particular EMG) processing, neuromuscular system modeling and myoelectric prosthesis control.

Guanglin Li (M'01-SM'06) received the B.S. and M.S. degrees in electrical engineering from Shandong University, Jinan, and the Ph.D. degree in biomedical engineering from Zhejiang University, Hangzhou, China, and completed the postdoctoral research associate in bioengineering at the University of Illinois at Chicago.

He joined the faculty of the Department of Electrical Engineering, Shandong University, where he was an Associate Professor since 1998. He worked as a Research Fellow and later as a Postdoctoral Research Associate in the Department of Bioengineering at the University of Illinois at Chicago from 1999 to 2002. After working as a Senior Research Scientist at BioTechPlex Corporation (2002 to 2006), he joined the Rehabilitation Institute of Chicago (RIC) and the faculty of Northwestern University (NU), Chicago, USA, where he is currently a Research Scientist in the Neural Engineering Center for Artificial Limbs at RIC and a Research Assistant Professor of Physical Medicine and Rehabilitation at NU. His current major research interests include multifunctional artificial arm control, neural-machine interface, biomedical signal analysis and computational biomedical engineering.

Todd A. Kuiken, (M'99-SM' 07) completed his BS in BME at Duke University, Durham, North Carolina in 1983. He received his PhD in BME (1989) and MD (1990) from Northwestern University, Chicago, IL. He completed his residency in Physical Medicine and Rehabilitation at the Rehabilitation Institute of Chicago and Northwestern University Medical School, Chicago, Illinois in 1995.

He is currently the Director of the Neural Engineering Center for Artificial Limbs and Director of Amputee Services at the Rehabilitation Institute of Chicago. He is an Associate Professor in the Depts. of PM&R and Biomedical Engineering of Northwestern University. He is also the Associate Dean, Feinberg School of Medicine, for Academic Affairs at the Rehabilitation Institute of Chicago.

Appendix. EMG Pattern Recognition Using Linear Discriminant Analysis

The movement classes were presented as C_g ($g \in [1, G]$), where G denotes the total number of classes. For each movement, the recorded EMG data were composed of 10 five-second active attempts, which were divided into 10 segments with a labelled attempt number from 1 to 10. The 5 EMG data segments with even numbers were assigned as the training data and the rest were used as testing data. In both sets, EMG signals were segmented into a series of analysis windows with a window length of 256 ms and a window increment of 64 ms. In each analysis window, four TD features of all applied bipolar EMG signals were extracted and concatenated to form an observation of feature vector: $\bar{f} = \{f_1, f_2, \ldots f_n, \ldots, f_N\}^T$. f_n consists of four TD features of the n bipolar EMG signal; N is the total number of applied bipolar EMG signals.

The idea of discriminant analysis is to classify the observed data to the movement class in which the posteriori probability $P(C_g|\bar{f})$ can be maximized [23]. The posteriori probability is the probability of class C_g given the observed feature vector $\bar{f}$ and can be expressed as

$$P(C_g|\bar{f}) = \frac{P(f|C_g)P(C_g)}{P(\bar{f})}, \quad (6)$$

where $P(C_g)$ is the priori possibility, $P(\bar{f}|C_g)$ is the likelihood, and $P(\bar{f})$ the possibility of observed feature vector $\bar{f}$. In this study, given movement class C_g, the observed feature vectors had a multivariate normal (MVN) distribution, i.e. $P(\bar{f}|C_g) \sim MVN(\mu_g, \Sigma_g)$, where μ_g is the mean vector and Σ_g is the covariance matrix of the class C_g. Additionally, the priori possibility was assumed to be equivalent for each movement class, i.e. $P(C_g) = {}^1\!/_G$. For simplicity, the logarithm was applied on both sides of (6). Since $P(\bar{f})$ and $P(C_g)$ were the same for every movement class in this study, both terms were ignored in the maximization of posteriori possibility as shown in (7).

$$\begin{aligned} \tilde{C}_g &= \arg\max_{C_g} \{\ln P(C_g|\bar{f})\} = \arg\max_{C_g} \{\ln P(\bar{f}|C_g)\} \\ &= \arg\max_{C_g} \{-\tfrac{1}{2}(\bar{f}-\mu_g)^T \textstyle\sum_g^{-1} (\bar{f}-\mu_g) - \tfrac{1}{2}\ln\|\textstyle\sum_g\|\}, \quad C_g \in [C_1, C_2, \ldots C_G]. \end{aligned} \quad (7)$$

By assuming that every class shared a common covariance, i.e. $\Sigma_g = \Sigma$, (7) can be further simplified as

$$\begin{aligned} \tilde{C}_g &= \arg\max_{C_g} \{\bar{f}^T \textstyle\sum^{-1} \mu_g - \tfrac{1}{2}\mu_g{}^T \textstyle\sum^{-1} \mu_g\} \\ &= \arg\max_{C_g} (d_{C_g}), \end{aligned} \quad (8)$$

where

$$d_{C_g} = \bar{f}^T \sum^{-1} \mu_g - \frac{1}{2}\mu_g{}^T \sum^{-1} \mu_g \quad (9)$$

was the linear discriminant function.

During the training procedure, μ_g and Σ were estimated by the feature vectors calculated from the training data.

$$\tilde{\mu}_g = \frac{1}{K_g}\sum_{k=1}^{K_g} \bar{f}_{C_g,k} \text{ and } \tilde{\sum} = \frac{1}{G}\sum_{g=1}^{G} \frac{1}{K_g - 1}(F_g - M_g)(F_g - M_g)^T$$

where K_g is the number of observations in class C_g; $\bar{f}_{C_g, k}$ is the k observed feature vector in class C_g; F_g is the feature matrix $F_g = [\bar{f}_{C_g, 1}, \bar{f}_{C_g, 2}, \ldots \bar{f}_{C_g, k}, \ldots, \bar{f}_{C_g, K_g}]$; M_g is the mean matrix $M_g = [\tilde{\mu}_g, \tilde{\mu}_g, \ldots \tilde{\mu}_g]$ that has the same number of columns as in F_g. Therefore, the parameters in the linear discriminant function (9) were known, i.e.

$$\tilde{d}_{C_g} = \tilde{f}^T \tilde{\sum}^{-1} \tilde{\mu}_g - \frac{1}{2}\tilde{\mu}_g{}^T \tilde{\sum}^{-1} \tilde{\mu}_g. \quad (10)$$

In the testing procedure, each observed feature $\bar{f}$ derived from the testing data set was applied to calculate $\tilde{d}_{C_g}$ in (10) for each movement class and was classified into a specific class $\tilde{C}_g$ that satisfied

$$\tilde{C}_g = \arg\max_{C_g} \{\tilde{d}_{C_g}\}, C_g \in \{C_1, C_2, \ldots, C_G\}.$$

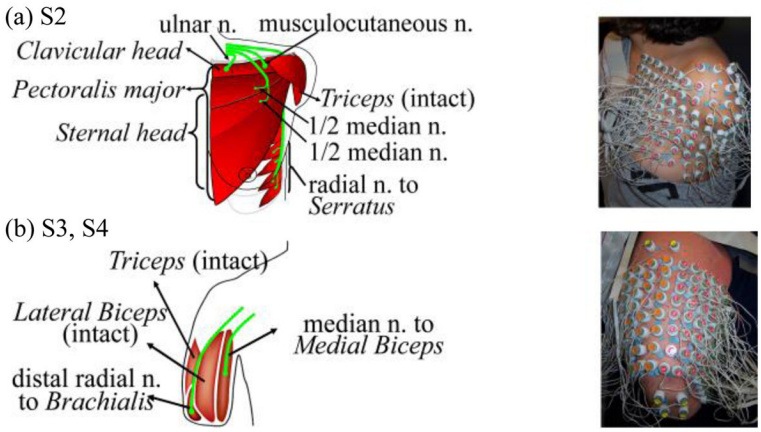

Fig. 1.

Schematic description of targeted muscle reinnervation techniques (left panel) and the high density EMG experimental setup (right panel) in (a) unilateral short transhumeral amputee subject S2, and (b) unilateral long transhumeral subjects S3 and S4. ‘n.’ denotes nerve.

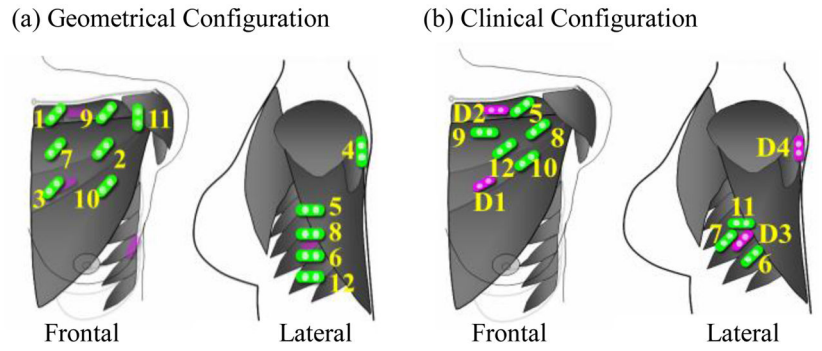

Fig. 2.

Schematic description of the selected electrodes in (a) Geometrical Configuration and (b) Clinical Configuration on subject S2. Purple electrodes demonstrate the direct control sites. Clinical Configuration utilizes direct control sites for the first four selected electrodes that are labeled D1 (hand close), D2 (elbow flexion), D3 (hand open), and D4 (elbow extension). Green electrodes indicate other applied electrodes. The labeled number beside the electrode indicates the sequence of electrode placement.

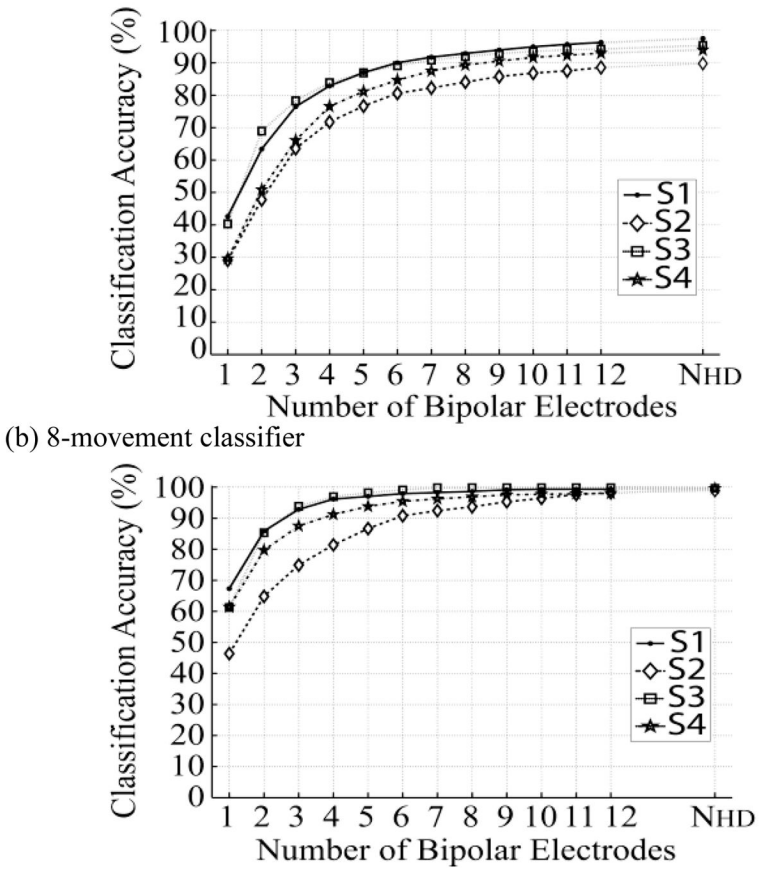

(b) 8-movement classifier

Fig. 3.

Classification accuracy of (a) 16-movement classifier and (b) 8-movement classifier when using different numbers of SFS-selected suboptimal electrodes. Results are from all four subjects. N_{HD} denotes the total number of bipolar electrodes derived from the high-density EMG array.

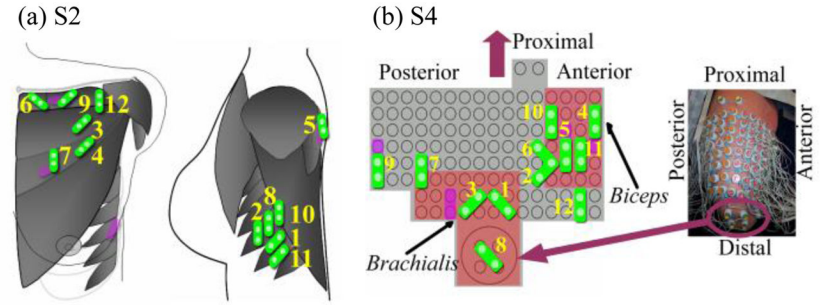

Fig. 4.

Schematic description of the Suboptimal Configurations for classifying 16 movements. The representative data are from (a) S2 and (b) S4. As points of reference, the purple electrodes demonstrate the locations of direct control sites. Green electrodes indicate the suboptimal electrodes. Each electrode is labeled with a number that indicates its sequence of selection using SFS.

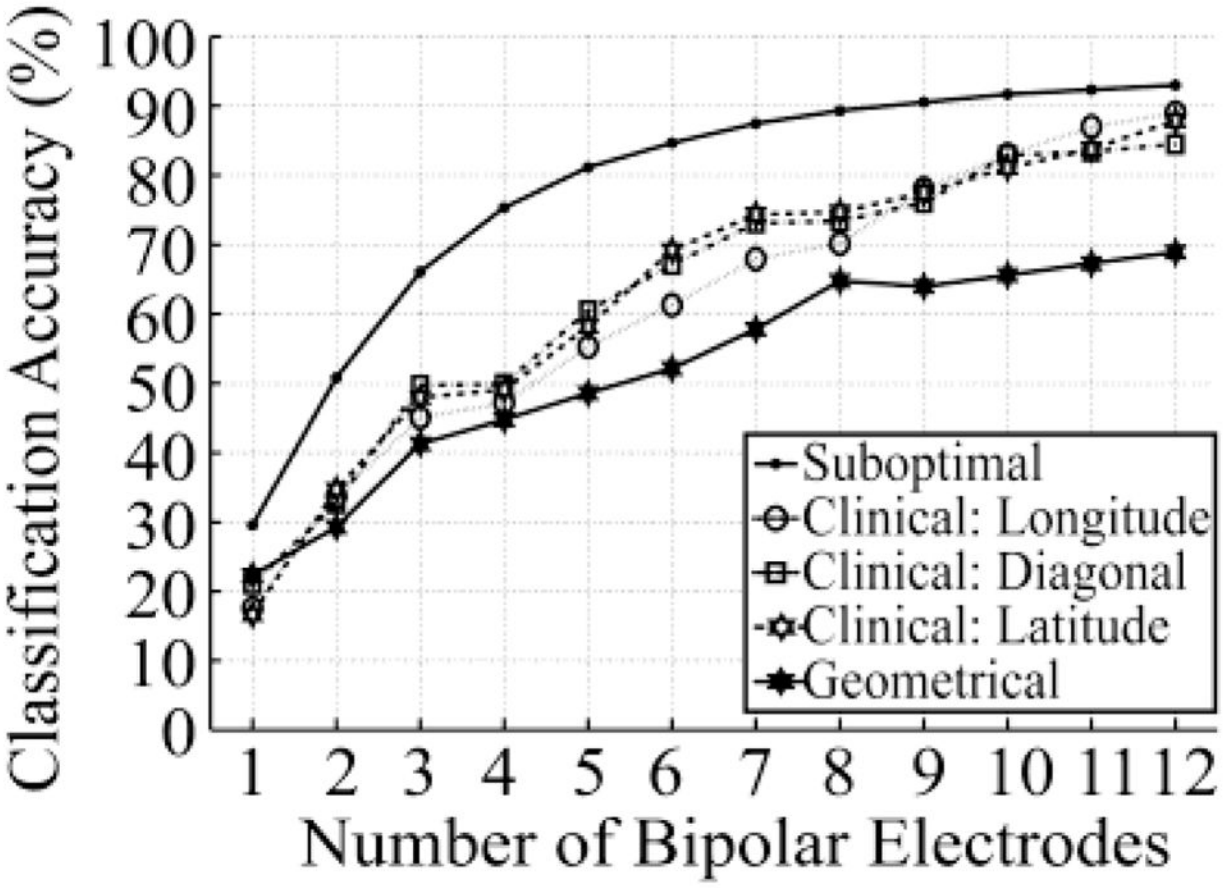

Fig. 5.

Comparison of classifier accuracy among different electrode configurations. Results are from S4. Compared configurations include Suboptimal Configuration, Clinical Configuration with longitudinal, latitudinal and diagonal electrode orientation, and Geometrical Configuration.

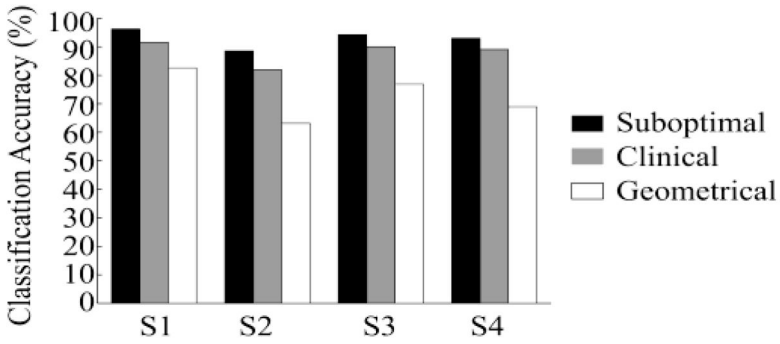

Fig. 6.

The accuracy of classifying 16 intended movements with 12 electrodes placed according to Suboptimal, Clinical, and Geometrical Configuration.